

T-Plots: A Novel Approach to Network Design

ITAMAR COHEN

T-Plots: A Novel Approach to Network Design

RESEARCH THESIS

In Partial Fulfillment of The Requirements for the Degree of Master
of Science in Electrical Engineering

ITAMAR COHEN

Submitted to the Senate of the Technion - Israel Institute of Technology
Kislev, 5768 Nov 2007

The research thesis was done under the supervision of Dr. Isaac Keslassy in the Faculty of Electrical Engineering.

I gratefully thank Dr. Isaac Keslassy for his dedicated supervision, for the continuous support and for the inspiring ideas.

I would like to thank also the computer networks lab team: Yoram Orchen, Yoram Yihyie and Hai Vortman, for the technical support.

The generous financial help of the Banin Fund and of Cisco Israel are gratefully acknowledged.

Contents

1	Introduction	1
1.1	Overview	1
1.2	Previous work	4
1.2.1	Dynamic routing changes	4
1.2.2	Oblivious routing algorithms	4
1.2.3	Traffic matrices and T-Sets	5
1.2.4	T-Plots	5
1.3	Outline of the Thesis	6
2	T-Plot model	7
3	T-Plots are #P-Complete	10
3.1	Edge T-Plots are #P-Complete	10
3.2	Global T-Plots are #P-Complete	13
4	Gaussian model	15
4.1	Finding the Gaussian parameters	15
4.2	Generalization to different T-Sets	16
4.2.1	Continuous T-Sets	16
4.2.2	Traffic matrices with diagonal 0	17

4.2.3	Heterogeneous T-Sets	18
4.3	Gaussian model example	19
4.4	To be or not to be (Gaussian)	20
4.4.1	When flows are i.i.d.	22
4.4.2	A counter-example	22
4.4.3	When the edge is overloaded	24
5	Congestion guarantees	25
6	Approximation and bounds of the global congestion CDF	29
7	Capacity allocation scheme	31
8	Simulations	33
8.1	T-Set representation	33
8.2	Experimental setup	35
8.3	Edge T-Plots	36
8.4	Global T-Plots	41
8.5	Improved capacity allocation	42
8.6	Heterogeneous network	44
9	Conclusion	46

List of Figures

1.1	Link load distribution on the (Kansas City, Indianapolis) link in Abilene network, when the T-Set is \mathcal{A}	2
4.1	Link load distribution on the (Seattle, Sunnyvale) link in Abilene network, when the T-Set is \mathcal{A}	20
4.2	Normal Probability Plots of the congestion on two edges in Abilene network (the T-Set is \mathcal{A})	21
4.3	PDF of the congestion for the scenario detailed in Sec. 4.4.2 (the T-Set is \mathcal{P})	23
5.1	Three views of the same T-Plot (edge 13, the T-Set is \mathcal{P})	26
5.2	Three views of the same T-Plot (edge 13, the T-Set is \mathcal{P} , T-Plot of the throughput).	27
8.1	PDF of the global congestion in the 2×2 cube (when the T-Set is \mathcal{A}) . . .	34
8.2	Abilene backbone network	35
8.3	Congestion PDF on e_{13} over discrete T-Sets	37
8.4	Congestion PDF on e_{13} over continuous T-Sets	38
8.5	Congestion PDF on e_1 over discrete T-Sets	39
8.6	Congestion PDF on e_1 over continuous T-Sets	40
8.7	Global congestion PDF: over \mathcal{A}	41
8.8	Global congestion CDF: bounds and improvements	43
8.9	PDF of the global congestion for the heterogeneous T-Set	45

Abstract

It is accepted wisdom that changes in the traffic matrix entail capacity over-provisioning, but there is no simple measure of just how much over-provisioning can buy. In this Thesis, we aim to provide the network designer with a simple view of the network robustness to traffic matrix changes. We first present the Traffic Load Distribution Plots, or T-Plots, a class of plots illustrating the percentage of traffic matrices that can be serviced as a function of the capacity over-provisioning. For instance, from a simple look at their T-Plots, network designers can guarantee that their network services all admissible traffic matrices, or 99% of permutation traffic matrices, or all traffic matrices with ingress/egress load at most half the maximum. We further show that, unfortunately, in the general case plotting T-Plots is $\#P$ -Complete, i.e., that it is impossible to plot a T-plot in a polynomial time by the noon tools. However, we show that T-Plots can sometimes be closely modeled as Gaussian, thus only using two values (mean and variance) to quantify the robustness of a capacity allocation to traffic matrix changes. We further utilize these Gaussian T-Plots to provide a more robust capacity allocation. Finally, we demonstrate the benefits of using T-Plots by showing results of extensive Monte Carlo simulations in a real backbone network.

This Thesis was submitted in 2007. Since then, the results that appeared in it were applied in various networking environments. In this newer version, we revisit the results 13 years later and explain their relevance to state-of-the-art problems in network design.

Chapter 1

Introduction

1.1 Overview

Network design aims to i) guarantee high throughput and low delay for current and future traffic demands, ii) minimize the amount of over-provisioned capacity and iii) minimize the number of dynamic routing changes, which cause undesired effects, such as out-of-order arrival of packets and drastic changes in traffic flows.

Balancing between these three goals, which often contradict each other, necessitates the usage of efficient, yet accurate, measurement tools. However, the development of such tools is a hard task, due to the frequent changes in traffic demands in state-of-the-art networks: a routing algorithm, while optimal for a typical traffic demand, might fare quite poorly as traffic conditions change.

The goal of this Thesis is to provide a common practical framework to evaluate and compare routing algorithms in the always-changing traffic demands environment. In addition, once the routing algorithm is chosen, the tools developed here enable a simple, yet efficient, capacity allocation scheme for achieving high throughput without wasting network resources.

The main contribution of this Thesis is the introduction of the *T-Plots*, or Traffic Load Distribution Plots, a class of plots illustrating the distribution of the load generated by the whole set of possible future traffic demands (called *T-Set*). The network operator first defines a routing algorithm, a link capacity allocation, and a T-Set that reflects the changes in traffic demand. Then, the operator can plot the load distribution and directly evaluate the efficiency of a traffic engineering approach according to some given metric

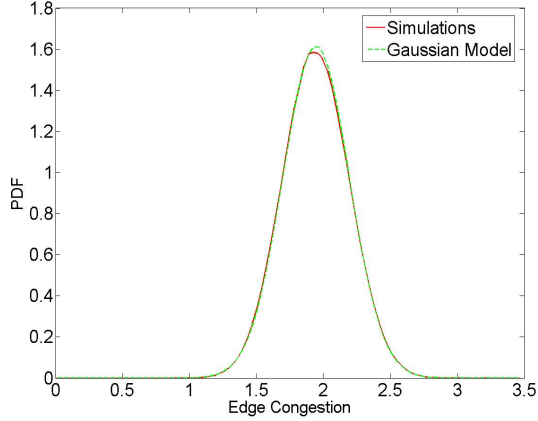


Figure 1.1: Link load distribution on the (Kansas City, Indianapolis) link in Abilene network, when the T-Set is \mathcal{A}

(e.g., average load, worst-case load, or 99%-cutoff load).

Figure 1.1 provides a T-Plot example. It shows the distribution of the normalized load on the loaded link in Abilene backbone network (details in Chapter 8) [1]. The T-Set is assumed to be the set \mathcal{A} of all admissible traffic matrices, (see Chapter 2). In this T-Plot, the average load is about 1.9, the 98%-cutoff load is about 2.5, and the worst-case load can be found to be exactly 5 (with a negligible density); in other words, this T-Plot shows that when capacity equals half of the worst-case load, 98% of the matrices in the T-Set can already be serviced. Thus, using this T-Plot, an operator can directly deduce the performance of its traffic engineering algorithm and obtain clear performance guarantees. The operator might decide, for instance, that the marginal benefit of allocating more capacity beyond 2.5 is not worth the cost. Incidentally, note that the T-Plot can be closely modeled as Gaussian – we will later develop on that point.

Depending on the problem faced, T-Plots can be considered in several ways. They mainly provide a theoretical analysis tool and a unified view of the different traffic engineering and capacity allocation algorithms. But they also constitute a practical day-to-day monitoring tool for network operators, who have a given topology and a given routing algorithm, and simply want to monitor the influence of traffic changes on their network performance. The way T-Plots are used and their associated T-Sets highly depend on the reasons underlying the changes in traffic demands.

In this Thesis, we set out to study the advantages and drawbacks of T-Plots. We first demonstrate that the exact computation of T-Plots is $\#P$ -Complete, thus killing early

hopes of easy results. Indeed, computing exact T-Plots on networks of more than five nodes proves extremely hard, if not impossible, when using standard tools like Vinci [41]. However, we propose a simple random-walk algorithm that provides a close approximation to the exact T-Plot, thus enabling us to study T-Plots in typical networks. Further, we also show that T-Plots can sometimes be closely modeled as Gaussian when using typical regular T-Sets. Therefore, the knowledge of two single values (mean and variance) is enough to provide a model of the whole load distribution and quantify the robustness of a capacity allocation scheme to traffic matrix changes. Further, we also determine exact simple bounds on the load distribution, thus enabling operators to provide strict performance guarantees over any T-Set. Further, we illustrate the possible use of T-Plots in optimization schemes, by providing a toy model for a capacity allocation scheme, in which the capacity provided to each link is equal to the sum of its average load and a multiple of the load standard deviation. Using a toy model of the Abilene backbone network, we show that such a simple scheme is surprisingly close to the performance bounds generated by the set of optimally robust capacity allocations.

We would like to stress that in our view, the key aspect of this work is the way it opens the road for future studies. Our results enable the research community to compare and judge algorithms along the same scale. Further, we show that there is more to look at in optimization algorithms than the average-case and the worst-case. Finally, we readily admit that it is yet unclear in what exact conditions T-Sets will yield Gaussian T-Plots; and, while we provide some intuition, we leave to future studies this fundamental question on traffic engineering models.

Some of our results also appear in [51, 52, 53]. These results were applied mainly in the context of Network-on-Chip, e.g., in [54]. However, over the years similar ideas were extensively studied also in other networking environments. For instance, the emergence of data-center-networks in recent years has increased the interest in developing oblivious routing algorithms with congestion guarantees in such networks [55]. Using a statistical approach for tackling uncertainty and heterogeneity in communication networks was studied in the context of buffering and scheduling [56, 57], scheduling [58, 59], and caching [60, 61, 63, 62].

1.2 Previous work

1.2.1 Dynamic routing changes

Dynamic routing algorithms try to perform routing changes which would minimize the probability that a link in the network would become overloaded [26, 27]. However, performing such routing changes requires full knowledge of the current and future traffic demands, which are in practice not available [8, 29, 50, 49]. In addition, routing changes cause undesired affects, such as out-of-order arrivals of packets and drastic changes in traffic flows.

1.2.2 Oblivious routing algorithms

Due to the practical problems when employing dynamic routing algorithms, many recent works discuss the optimization of oblivious routing algorithms, i.e. algorithms in which the routing between each (source, sink) pair of nodes is determined in advance, and doesn't change over time. Most works use the congestion in the network as the optimization criterion, and prove theoretical bounds on the ratio between the performances that an oblivious routing algorithm can achieve and those of an optimal adaptive routing algorithm [24, 9, 25, 11, 38]. Other objective functions are the amount of capacity over-provisioning [50, 38], and the length of the routing paths [21, 38]. Other works generalize the optimization criterion for a general function of the total flow on each edge in the network, where this function obeys some requirements (e.g. being concave) [23, 6, 46].

A promising class of network architectures are those based on Valiant Load Balancing (VLB) [39, 50, 29, 49]. VLB guarantees a constant throughput, even at traffic changes. The drawbacks of VLB schemes are that they typically entail longer routing paths, and require larger network resources. [31] proposes an enhancement to VLB that somewhat overcomes these drawbacks, but it assumes additional knowledge about the current traffic in the network, thus hurting the simplicity and easiness of implementation.

In practice, oblivious routing algorithms may also perform dynamic routing changes due to failures of links or nodes in the network. Some works aim to improve the resilience of network architecture, that deploy oblivious routing algorithms. The objective is to minimize the amount of over-provisioning used for guaranteeing restoration from failures [28, 5], and to minimize the number of dynamic routing changes due to each link failure [7].

Some works suggest hybrid algorithms, in which the baseline routing is oblivious, but it may change over time, aiming to reduce the congestion in the network [34] or the length of the routing paths [31].

1.2.3 Traffic matrices and T-Sets

A *traffic matrix* is a non-negative matrix, where the rows represent the sources, and the columns represent the destinations (formal definitions of all the terms used in the introduction appear in Chapter 2).

When evaluating an oblivious routing algorithm, one should consider its performances over the set of allowable traffic matrices (which we call *T-Set*). Several T-Set models have been proposed in the literature. The chosen T-Set is often the set \mathcal{A} of all admissible traffic matrices, i.e. of row/column sums bounded by the ingress/egress capacity, which are typically normalized to one (homogeneous case), as popularized by the hose model [16, 29, 17, 36]. Some works also focus on the set \mathcal{P} of permutation matrices [38, 33, 34], since in the homogeneous case the worst-case admissible traffic matrices are permutations [37], and every admissible traffic matrix can be represented as a linear combination of permutation matrices [12, 42]. Other approaches rely on historical traffic matrix values, for instance, based on one-hour window observations [4, 16], on critical matrices among those observed [48], on estimated traffic matrices [32], or on the sum of a typical traffic matrix and small fluctuations [8]. [8] also suggests methods for modeling a typical traffic matrix. However, the models proposed in [8] implicitly assume that the entries in the traffic matrix are independent. This assumption is used in traditional network design schemes, which use the pipe model, but it doesn't hold in networks that deploy the hose model [36, 16]. Finally, one can refer to [47] as to the tradeoffs involved in determining the size of the T-Set.

1.2.4 T-Plots

The reference that is most related to T-Plots in backbone networks appears to be [17]. [17] implicitly discusses the link between the CDF (Cumulative Distribution Function) of the global congestion and the required amount of overprovisioning in networks. In interconnection networks, several studies have presented plots of the throughput PDF (Probability Density Function) [33, 38, 34], but mainly as a mean for finding the average-case throughput and without real interest in the whole distribution. In this Thesis, we extend these results by modeling and bounding the whole distribution (and not merely the

average-case and worst-case) and showing its high importance for analyzing the network performances and optimizing the capacity allocation.

1.3 Outline of the Thesis

This Thesis is structured as follows. We formulate the T-Plot model in Chapter 2, and prove its $\#P$ -completeness in Chapter 3. Then, in Chapters 4 and 5, we provide a Gaussian view of the edge T-Plots, as well as strict performance, guarantees, and generalize these results to global T-Plots in Chapter 6. Finally, in Chapter 7, we introduce a simple capacity allocation scheme, which we evaluate, together with the other results, in Chapter 8.

Chapter 2

T-Plot model

We will now introduce the notations used to define T-Sets and T-Plots.

Network – Consider a directed graph $G(V, E)$ with $n=|V|$ nodes and $|E|$ edges. Node i may initiate traffic at a rate up to r_i , and receive traffic at a rate up to q_i . For simplicity of presentation we assume that $r_i = q_i = 1$ for all i (normalized homogeneous case), and will later explain how to extend this simplistic model to the general case. Each edge e is allocated a positive capacity $c(e) > 0$. We will say that an edge e is a *strictly minimal edge* if $c(e') > c(e)$ for each edge e' different from e , and a *bridge* if removing e would increase the number of components in the graph.

T-Set – A *traffic matrix* is an $n \times n$ non-negative matrix, where the entry in the location (i, j) represents the amount of traffic from node i to node j . We are interested in analyzing the network performance when traffic matrices belong to different Traffic Matrix Sets (T-Sets). For instance, typical T-Sets include:

- $\mathcal{A}(n)$, the set of all the doubly-substochastic traffic matrices, i.e. the $n \times n$ non-negative matrices for which each row and column sum is at most 1:

$$(2.0.1) \quad \mathcal{A}(n) = \left\{ D \mid \forall i, j : 0 \leq D_{ij} \leq 1, \sum_j D_{ij} \leq 1, \sum_j D_{ji} \leq 1 \right\}$$

In this work we use $\mathcal{A}(n)$ interchangeably with *all admissible traffic matrices*.

- $\mathcal{S}(n)$, the set of doubly-stochastic traffic matrices (i.e. $n \times n$ non-negative matrices for

which the row and column sums equal exactly 1):

$$(2.0.2) \quad \mathcal{S}(n) = \left\{ D \mid \forall i, j : 0 \leq D_{ij} \leq 1, \sum_j D_{ij} = 1, \sum_j D_{ji} = 1 \right\}$$

- $\mathcal{P}(n)$, the discrete set of $n!$ permutations (i.e. the set of $n \times n$ 0-1 matrices with exactly single 1 in each row and column):

$$(2.0.3) \quad \mathcal{P}(n) = \left\{ D \mid \forall i, j : D_{ij} \in \{0, 1\}, \sum_j D_{ij} = 1, \sum_j D_{ji} = 1 \right\}$$

$\mathcal{A}(n)$, which is defined by a set of linear inequalities, forms a convex polytope, also known as “the routing polytope” [6]. $\mathcal{S}(n)$, which is defined by a set of linear equalities, forms the faces of the polytope $\mathcal{A}(n)$ (it is easy to think of it as the *surface* around $\mathcal{A}(n)$). $\mathcal{P}(n)$ is the discrete set of the vertices of this polytope [14]. The worst-case traffic matrices in $\mathcal{A}(n)$ are found within $\mathcal{P}(n)$ [37].

When there is no ambiguity, we shall use \mathcal{A} , \mathcal{S} and \mathcal{P} instead of $\mathcal{A}(n)$, $\mathcal{S}(n)$ and $\mathcal{P}(n)$, respectively.

In the remainder, we will assume that traffic matrices are selected u.a.r. (uniformly at random) from the T-Set, but this can of course easily be extended to weighted T-Sets by using a weighted metric over the T-Set metric space, so that the probabilities of choosing each traffic matrix correspond to these weights.

Routing – A *routing* is classically defined as a set of $n^2|E|$ variables $\{f_{ij}(e)\}$, where $f_{ij}(e)$ denotes the fraction of the traffic from node i to node j that is routed through edge e . The routing is assumed to satisfy the classical linear flow conservation constraints [9]. Such a routing is oblivious in the sense that the routing variables are independent of the current traffic matrix. Note that the routing is allowed to depend on both the source and the destination, as in MPLS, and therefore subsumes routings that only depend on the destination, as in many Interior Gateway Protocols [46, 47].

Congestion – The total *flow* crossing an edge $e \in E$ when routing the traffic matrix D is $F(e, f, D) = \sum_{i,j} D_{ij} f_{ij}(e)$, where D_{ij} is the $(i, j)^{\text{th}}$ element of matrix D . Then, the *edge congestion* on edge e is equal to the total flow crossing it divided by the edge capacity, i.e.

$$(2.0.4) \quad EC(e, f, D) = \frac{F(e, f, D)}{c(e)} = \frac{\sum_{i,j} D_{ij} f_{ij}(e)}{c(e)}$$

Thus, when the edge congestion on e is at least 1, the flow crossing e is not below its capacity, and we will say that e is *saturated*. Further, a network is saturated if at least one edge in it is saturated. The *global congestion* of routing D using f will be obtained by maximizing the edge congestion over all the edges, that is:

$$(2.0.5) \quad GC(f, D) = \max_{e \in E} \{EC(e, f, D)\}$$

In this thesis, congestion and load are used interchangeably.

For a saturated network, the *throughput* is defined as the inverse of the global congestion, and is otherwise made not to exceed 100%:

$$(2.0.6) \quad TP(f, D) = \min\{GC(f, D)^{-1}, 1\}$$

T-Plot – T-Plots (the Traffic Load Distribution Plots) can be classified into two categories: *edge T-Plots*, which show the distribution of an edge congestion generated by traffic matrices in the T-Set; and *global T-Plots*, which similarly show the distribution of the global congestion generated by traffic matrices in the T-Set. T-Plots can be represented in a CDF (Cumulative Distribution Function) or PDF (Probability Distribution Function) way. For example, the value of the *edge T-plot CDF* at point L is the probability that the edge congestion imposed on that edge by a traffic matrix selected u.a.r. from the T-Set would be at most L :

$$(2.0.7) \quad EC_{CDF}^T(e, f, L) = \Pr \{EC(e, f, D) \leq L | D \in T\}$$

Likewise, it is possible to use the *edge T-plot PDF*, which corresponds to the derivative of the CDF whenever it exists. (For simplicity, we shall use the same terms for both discrete and continuous T-Sets.) The CDF and PDF of the *global congestion* are, of course, defined similarly.

Given an edge T-Plot, it is easy to find the *worst-case edge congestion*, as well as statistics such as the *average-case edge congestion* and the *variance* of the edge congestion, which are computed over the whole T-Set using a uniform measure on that metric space.

Chapter 3

T-Plots are #P-Complete

Now that we have introduced T-Plots, we will prove that their computation is #P-C. We will first show it for *edge T-Plots*, which display the congestion distribution on a given edge, and then as well for *global T-Plots*, which plot the distribution of the global congestion. In both cases, we reduce the problem of computing the permanent of a 0-1 matrix, which is known for being #P-complete, to a specific T-Plot computation problem with a specific T-Set. Thus, by showing that a specific T-Plot computation problem is #P-complete, we demonstrate that the general computation of an arbitrary T-Plot is #P-complete as well.

3.1 Edge T-Plots are #P-Complete

Before proving that the computation of edge T-Plots is #P-Complete, we need some preliminaries[10].

Definition 1 *Let f be a function. We say that $f \in \#P$ if there exists a binary relation R s.t.*

- If $(x, y) \in R$ then the length of y is polynomial in the length of x .
- It can be verified in polynomial time that a pair (x, y) is in R .
- For every $x \in \Sigma^*$ (the set of all 0-1 strings), $f(x) = |\{y : (x, y) \in R\}|$

Definition 2 *Given two functions f, g*

- There is a *polynomial Turing-reduction* from g to f (and denote $g \propto f$) if the function g can be computed in polynomial time using an oracle to f .
- A function $f : \Sigma^* \rightarrow N$ is *#P-Hard* if for every $g \in \#P$ there is a polynomial reduction $g \propto f$.
- A function f is *#P-Complete* if it is both *#P-Hard* and in *#P*.

Definition 3 Given an $n \times n$ matrix A , the permanent of A is defined as

$$(3.1.1) \quad \text{Perm}(A) = \sum_{\sigma \in \mathcal{P}(n)} \prod_{i=1}^n A_{i,\sigma(i)}$$

We denote the problem of computing the permanent of a 01-matrix as *01-Perm*. It was shown in [10] that 01-Perm is #P-Complete.

Lemma 1 Let $G(V, E)$ be a connected graph. Let e be a non-bridge edge. Then, for each pair of nodes (s, d) , there exists at least one walk, which uses e exactly once, and at least one additional walk, which doesn't use e .

Proof. Let's denote $e = (a, b)$. Since e is not a bridge, for each (source, destination) pair of nodes (s, d) , there exists a walk that doesn't use e . Let's also construct a walk from s to d that uses e exactly once. First, from s to a , we use a walk that doesn't use e (such a walk exists, because e is not a bridge) Then, from a to b , we cross through e . Finally, from b to d , we use another walk that doesn't use e (again, such a walk exists, because e is not a bridge).

We will Theorem 1 by showing that the problem is #P (Lemma 2), and then showing a polynomial-time reduction from the problem of *01-Perm* (Lemma 3).

Intuitively, given an $n \times n$ matrix A and a non-bridge edge e , this reduction computes a routing algorithm f that routes packets from source s to destination d via e iff $A_{sd} = 1$. We will show that as a consequence, the value of the permanent of A is equal to the number of permutations, for which all the flow is routed via e . Therefore, using this equality, an oracle to a specific point of the PDF of the congestion on e suffices for calculating the permanent of A .

Lemma 2 Let $G(V, E)$ be a directed graph, in which the traffic is routed according to an oblivious routing algorithm f . Let e be a non-bridge edge. Then, $EC_{PDF}^P(e, f, L)$ is in #P.

Proof. Let us denote $L = \frac{n}{c(e)}$. Let's define the binary relation R as follows:

$$(3.1.2) \quad ((e, f, L), \sigma) \in R \Leftrightarrow EC(e, f, \sigma) = L$$

- The size of the representation of a permutation is polynomial in the representation of (e, f) .
- It can be verified in polynomial time whether $((e, f, L), \sigma) \in R$ by calculating $EC(e, f, \sigma)$.
- As $EC_{PDF}^{\mathcal{P}}(e, f, L)$ represents the probability of a randomly chosen permutation to impose congestion L on edge e , and $|\mathcal{P}(n)| = n!$,

$$(3.1.3) \quad n!EC_{PDF}^{\mathcal{P}}(e, f, L) = |\{\sigma \in \mathcal{P}(n) : EC(e, f, \sigma) = L\}|$$

Note that the multiplication by $n!$ doesn't affect $EC_{PDF}^{\mathcal{P}}(e, f, L)$ being in $\#P$.

Lemma 3 *Let A be an $n \times n$ 01-matrix. Let σ be a permutation of $\{1, 2, \dots, n\}$. Then, it is possible to construct in polynomial time a routing algorithm f s.t.*

$$(3.1.4) \quad \prod_{i=1}^n A_{i, \sigma(i)} = 1 \Leftrightarrow EC(e, f, \sigma) = L$$

Proof. We will construct an oblivious routing algorithm f s.t.

$$(3.1.5) \quad \forall i, j \in V : f_{ij}(e) = A_{ij}$$

In other words, if $f_{sd}(e) = 1$, f will use e exactly once when routing packets from s to d . Otherwise, f will not use e when routing packets from s to d . By the construction:

$$(3.1.6) \quad \begin{aligned} \prod_{i=1}^n A_{i, \sigma(i)} = 1 &\Leftrightarrow \sum_{ij} \sigma_{ij} A_{ij} = n \\ &\Leftrightarrow \sum_{ij} \sigma_{ij} f_{ij}(e) = n \\ &\Leftrightarrow EC(e, f, \sigma) = \frac{n}{c(e)} = L \end{aligned}$$

If $A_{sd} = 0$, f routes the packets from s to d via a walk, which does not use e . Else, f routes the packets from s to d via a walk which uses e exactly once, as described in the proof of Lemma 1. f can be calculated by running the Dijkstra Algorithm [3] n times on the graph $G'(V, E \setminus \{e\})$, each time taking a different node in the graph as the source node. Each edge in $E \setminus \{e\}$ has a unit weight. The complexity of the construction is polynomial, as it requires $O(|V|)$ runs of the Dijkstra Algorithm, where each run takes polynomial time.

Theorem 1 *When the T-Set is the set of permutations \mathcal{P} , finding the edge T-Plot of a non-bridge edge e is $\#P$ -C.*

Proof. Let A be a $n \times n$ 01-matrix. By Lemma 2, $EC_{PDF}^{\mathcal{P}}(e, f, L)$ is $\#P$. Successively using Lemma 3 and (3.1.3):

$$\begin{aligned}
 (3.1.7) \quad Perm(A) &= |\{\sigma \in \mathcal{P}(n) : \prod_{i=1}^n A_{i,\sigma(i)} = 1\}| \\
 &= |\{\sigma \in \mathcal{P}(n) : EC(e, f, \sigma) = L\}| \\
 &= n! EC_{PDF}^{\mathcal{P}}(e, f, L)
 \end{aligned}$$

This is a polynomial reduction from $01Perm$ to $EC_{PDF}^{\mathcal{P}}$. As $01Perm$ is $\#P$ -Hard, $EC_{PDF}^{\mathcal{P}}$ is $\#P$ -C, where even the task of computing the value of the distribution at an arbitrary point is $\#P$ -C. Consequently, $EC_{CDF}^{\mathcal{P}}$ is $\#P$ -C as well.

Corollary 1 *In the general case, finding the edge T-Plot is $\#P$ -C.*

3.2 Global T-Plots are $\#P$ -Complete

We have just proved that finding the edge T-Plot is $\#P$ -C. We shall now prove that finding the global T-Plot is $\#P$ -C as well.

In a network with a strictly minimal edge e_m , the worst-case congestion on e_m is higher than the worst-case congestion on any other edge in the network. Thus, e_m 's worst-case edge congestion is equal to the network's *global* congestion. Thus, similar construction to that used in Section 3.1 would suffice to prove that $GC_{CDF}^{\mathcal{P}}$ is $\#P$ -C as well.

Theorem 2 *When the T-Set is the set of permutations \mathcal{P} , finding the global T-Plot of a graph that includes a strictly minimal edge is $\#P$ -C.*

Proof. Let us denote: $L = \frac{n}{c(e_m)}$. Let A be a $n \times n$ 01-matrix. $GC(f, L) \in \#P$ by the same proof as that of Lemma 2. By Lemma 3, there exists a polynomial-time construction of a routing algorithm f s.t.

$$(3.2.8) \quad \prod_{i=1}^n A_{i,\sigma(i)} = 1 \Leftrightarrow EC(e_m, f, \sigma) = L$$

As e_m is strictly minimal, its worst-case congestion is higher than the worst-case congestion on every other edge, and therefore its worst-case edge congestion is equal to the network's

global congestion. We finally get:

$$(3.2.9) \quad \forall \sigma \in \mathcal{P}(n), \forall e \in E, e \neq e_m : EC(e, f, \sigma) \leq \frac{n}{c(e)} < L$$

And thus e_m 's worst-case edge congestion is equal to the network's *global* congestion

$$(3.2.10) \quad GC(f, \sigma) = L \Leftrightarrow EC(e_m, f, \sigma) = L$$

By combining Equations (3.1.7) and (3.2.10):

$$Perm(A) = n!EC_{PDF}^{\mathcal{P}}(e_m, f, L) = n!GC_{PDF}^{\mathcal{P}}(f, L)$$

As in the proof of Theorem 1, even the task of computing the value of $GC_{PDF}^{\mathcal{P}}$ at an arbitrary point is $\#P$ -C. Consequently, $GC_{CDF}^{\mathcal{P}}$ is $\#P$ -C as well.

Corollary 2 *In the general case, finding the global T-Plot is $\#P$ -C.*

We have proved that the exact computation of T-Plots is $\#P$ -Complete, regarding local congestion as well as global congestion. This is reflected by the extreme complexity in computing exact T-Plots for networks of reasonable size. For instance, given a maximum algorithm running time of one day, we could not compute exact T-Plots even on a simple 3-by-2 network when using Vinci [41], a standard convex-polytope volume computation tool. An underlying reason behind this complexity is that computing the T-Plot is equivalent to multiple polytope volume computations — this number even being infinite in the case of continuous T-Sets — and polytope volume computations are $\#P$ -C in the general case [18]. Therefore, even getting exact values of T-Plots at fixed bins proves extremely hard. In fact, as the space dimension grows, [19] shows that we cannot hope for a good approximation when using a deterministic algorithm unless we take exponentially many points, and the best possible approximation of any polynomial-time algorithm is at least exponential in the space dimension. T-Plot computation is made even harder by the fact that the number of dimensions in the volume computation is equal to the number of flows, hence growing like $O(n^2)$ and not like $O(n)$. Consequently, there is not much to be done to make exact computation easier. Since exact T-Plot computation proves elusive, we can only try to approximate or bound it. This will be a recurring theme in this Thesis.

Chapter 4

Gaussian model

We just proved that in the general case, it is $\#P-C$ to find the edge T-Plots. Therefore, we will strive to look for a good approximation. We will now show that edge T-Plots can sometimes be closely modeled as Gaussian, so that it suffices to compute two single values (average and variance) to approximate them. We will first present how the average and the variance of the edge congestion can be found, and then study the Gaussian approximation based on these two values.

4.1 Finding the Gaussian parameters

Our objective is to compute the Gaussian parameters of the T-Plot of a given edge over a given T-Set. Later in this chapter, we will show that the general computation of these parameters can often be done by pre-computing once several T-Set-dependent values (e.g., average value for flow (i, j)), and then plugging in those fixed values each time simulation parameters are changed (e.g., a new routing function). Moreover, in several regular T-Sets, this computation is much simplified. We will present below the results of this computation when the chosen T-Set is the set of permutations \mathcal{P} . In that case, the average-case edge

congestion on edge e using routing f is:

$$\begin{aligned}
EC_{ac}^{\mathcal{P}}(e, f) &= \frac{1}{n!} \sum_{\sigma \in \mathcal{P}} EC(e, f, \sigma) \\
&= \frac{1}{n!} \sum_{\sigma \in \mathcal{P}} \frac{\sum_{ij} \sigma_{ij} f_{ij}(e)}{c(e)} \\
&= \frac{1}{n!c(e)} \sum_{ij} f_{ij}(e) \sum_{\sigma \in \mathcal{P}} \sigma_{ij} \\
(4.1.1) \quad &= \frac{1}{nc(e)} \sum_{ij} f_{ij}(e),
\end{aligned}$$

where the last equality relies on the fact that a given flow (i, j) is only used in $\frac{1}{n}$ th of the permutations. Likewise, the variance is calculated using the formula

$$(4.1.2) \quad Var_{\sigma \in \mathcal{P}}[EC(e, f, \sigma)] = E[EC(e, f, \sigma)^2] - E^2[EC(e, f, \sigma)],$$

with

$$(4.1.3) \quad E[EC(e, f, \sigma)^2] = \frac{1}{n!c(e)^2} \sum_{ijkl} f_{ij}(e) f_{kl}(e) \left(\sum_{\sigma \in \mathcal{P}} \sigma_{ij} \sigma_{kl} \right),$$

where the expectations are with respect to the random variable $\sigma \in \mathcal{P}$. By basic combinatorial considerations:

$$(4.1.4) \quad \sum_{\sigma \in \mathcal{P}} \sigma_{ij} \sigma_{kl} = \begin{cases} (n-1)! & i = k \wedge j = l \\ (n-2)! & i \neq k \wedge j \neq l \\ 0 & (i = k \wedge j \neq l) \vee (i \neq k \wedge j = l) \end{cases}$$

Therefore, it is possible to plug in these fixed values and directly compute the exact mean and variance for any edge e , capacity allocation $c(e)$ and routing algorithm f .

4.2 Generalization to different T-Sets

We will present below methods for computing the average and the variance of the load for various T-Sets.

4.2.1 Continuous T-Sets

We are now interested in demonstrating how the Gaussian parameters can be computed in typical continuous T-Sets. We will provide examples when the T-Sets are \mathcal{S} or \mathcal{A} , using the same techniques as in Section 4.1.

First, the average-case edge congestion is the average congestion caused by a matrix D selected u.a.r. in the T-Set T :

$$(4.2.5) \quad EC_{ac}^T(e, f) = \frac{\int_T EC(e, f, D) ds}{\int_T 1 ds},$$

with the simplified formula:

$$(4.2.6) \quad \begin{aligned} \int_T EC(e, f, D) ds &= \frac{1}{c(e)} \int_T \sum_{ij} [D_{ij} f_{ij}(e)] ds \\ &= \frac{1}{c(e)} \sum_{ij} f_{ij}(e) \int_T D_{ij} ds \end{aligned}$$

In the T-Set \mathcal{S} , the value of $\int_T D_{ij} ds$ is independent of i, j . There exist n^2 different pairs of (i, j) and $\sum_{ij} \int_{\mathcal{S}} D_{ij} ds = \int_{\mathcal{S}} \sum_{ij} D_{ij} ds = \int_{\mathcal{S}} n ds = n \int_{\mathcal{S}} 1 ds$. Hence $\int_{\mathcal{S}} D_{ij} ds = \frac{1}{n} \int_{\mathcal{S}} 1 ds$, and the average congestion is finally simply $EC_{ac}^T(e, f) = \frac{1}{nc(e)} \sum_{ij} f_{ij}(e)$.

When the T-Set is \mathcal{A} , it is possible to predetermine the value of $\int_T D_{ij} ds$ by Monte Carlo simulations with an arbitrary small error, as explained in Chapter 8. As this value depends only on n (and not on the topology or the routing algorithm), it is sufficient to precompute at most one such simulation for each qualified network.

The variance of the edge congestion is calculated as in Equations (4.1.2) and (4.1.3):

$$(4.2.7) \quad E_T[EC(e, f, D)] = \frac{1}{nc(e)^2} \sum_{ijkl} f_{ij}(e) f_{kl}(e) \int_T D_{ij} D_{kl} ds$$

By separating the mutual relations of i, j, k, l to the same 3 cases as in (4.1.4), it is possible to predetermine the value of $\int_T D_{ij} D_{kl} ds$ by Monte Carlo simulations - again, using at most one simulation for each qualified network.

4.2.2 Traffic matrices with diagonal 0

For the sake of completeness, please note that it is possible to add the assumption that a node cannot send traffic to itself, i.e. the entries of the traffic matrix diagonal will be 0. (Some works in the literature assume it [17, 9], while others do not [37, 33, 38, 34].) We denote by \mathcal{P}_d , \mathcal{S}_d and \mathcal{A}_d the 0-diagonal subsets of \mathcal{P} , \mathcal{S} and \mathcal{A} , respectively.

The *average edge congestion* when T-Set is \mathcal{P}_d is

$$(4.2.8) \quad EC_{ac}^{\mathcal{P}_d}(e, f) = \frac{1}{(n-1)c(e)} \sum_{ij} f_{ij}(e)$$

For calculating the variance of the edge congestion we will use again Equation (4.1.2), where the value of $E_{\mathcal{P}_d}[L^2]$ is computed using Equation (4.1.3):

$$(4.2.9) \quad E_{\mathcal{P}_d}[L^2] = \frac{n}{|\mathcal{P}_d(n)| * c(e)} \sum_{ijkl} f_{ij}(e) f_{kl}(e) \sum_{\sigma \in \mathcal{P}_d} \sigma_{ij} \sigma_{kl}$$

By basic combinatorial considerations:

$$(4.2.10) \quad \frac{n}{|\mathcal{P}_d(n)|} \sum_{\sigma \in \mathcal{P}_d} \sigma_{ij} \sigma_{kl} = \begin{cases} \frac{1}{n-1} & i = k \wedge j = l \\ 0 & (i = k \wedge j \neq l) \vee (i \neq k \wedge j = l) \\ \frac{1}{(n-1)(n-2)} & i \neq k \wedge j \neq l \end{cases}$$

When the T-Set is \mathcal{S}_d or \mathcal{A}_d , the average and the variance of the edge congestion may be calculated using Equations (4.1.2) and (4.2.6). Note that

$$\int_{\mathcal{S}_d} EC(e, f, D) ds = \frac{1}{n-1} \sum_{ij} f_{ij}(e)$$

The rest of the integrals may be calculated by Monte Carlo simulations, as detailed in Section 4.2.1.

4.2.3 Heterogeneous T-Sets

In our model, node i may initiate traffic at rate up to r_i , and receive traffic at rate up to q_i . At *heterogeneous* traffic models, there exists i s.t. $r_i \neq q_i$, or there exist i, j s.t. $r_i \neq r_j$ or $q_i \neq q_j$.

A general heterogenous T-Set H is a convex polytope:

$$(4.2.11) \quad H(n) = \left\{ D | \forall i : D_{ij} \geq 0, \sum_j D_{ij} \leq r_i, \sum_j D_{ji} \leq q_i \right\}$$

Note that the *surface* of this polytope creates an additional T-Set, in which the inequalities in (4.2.11) are replaced by equalities.

Let D be a traffic matrix in a heterogeneous T-Set H . The average and the variance of the edge congestion in D may be calculated by methods similar to those detailed in Section 4.2.1. Note that as the values of the entries in D are not identically distributed anymore, using Equation (4.2.5) requires at the worst-case calculating the integral $\int_T D_{ij} ds$ separately for each pair (i, j) , i.e. n^2 times. Using Equation (4.2.7) requires calculating up to n^4 integrals - one for each chosen 4 indices $(i, j, k, l) \in [1, n]^4$. However, recall that it is sufficient to calculate each of these integrals at most once for each qualified network.

4.3 Gaussian model example

In order to study the Gaussian model, we now present two typical examples of T-Plots of the normalized link congestion on our simplified model of the Abilene backbone network (details in Chapter 8). The T-Set is assumed to be the set \mathcal{A} of all admissible traffic demand matrices.

Consider Figure 1.1, already mentioned in the Introduction. Figure 1.1 shows the PDF of the edge congestion on the most-loaded Abilene edge, e_{13} , which corresponds to the (Kansas City, Indianapolis) directed edge (by symmetry, there is the same T-Plot for the reverse direction of the link). As can be seen, the fit of the Gaussian model is excellent. (As explained in Sections 4.2.1 and 8.1, the Gaussian plot is generated using an independent random-walk sampling algorithm to find the mean and variance; running more samples or taking the mean and variance from the simulations plot would simply make the two plots undistinguishable).

Now consider Figure 4.1, a plot of the edge congestion PDF on the *least-loaded* Abilene edge e_1 , corresponding to the (Seattle, Sunnyvale) link. Here the Gaussian model fares poorer. Note that it would also not work much better if we were to compensate for the hidden negative congestion values in the left of the Gaussian distribution by multiplying the positive right side of the PDF by some constant. This example shows that there is simply no guarantee that the Gaussian approximation will always work.

To check that the graphs indeed exhibit different behaviors, we tested both plots for normality by using two different methods. First, Figure 4.2 shows their corresponding Normal Probability Plots (NPPs). NPPs are a graphical technique for assessing whether or not a dataset is approximately normally distributed [13]. These NPPs were obtained

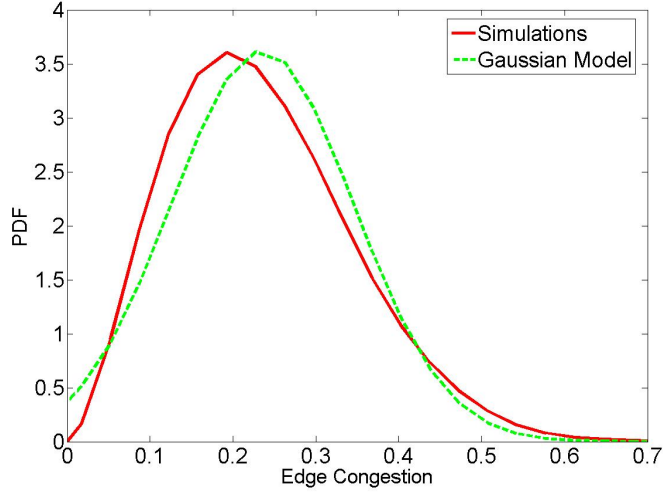


Figure 4.1: Link load distribution on the (Seattle, Sunnyvale) link in Abilene network, when the T-Set is \mathcal{A}

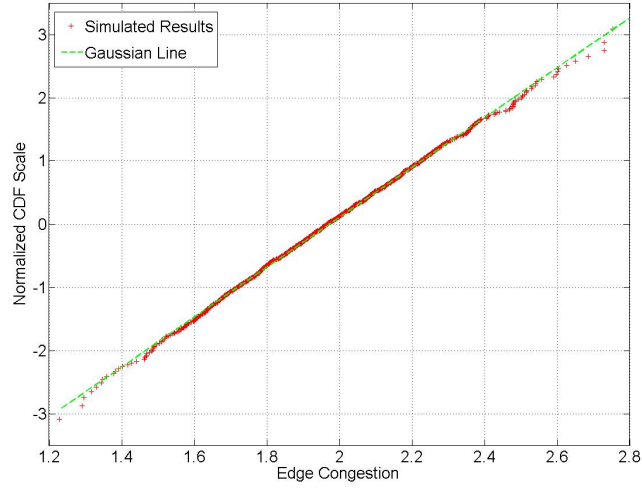
by running 1,000 samples, each time measuring the induced edge congestion, and then displaying the CDF of the sampled dataset, where the y-axis is scaled so that a normally distributed dataset would yield an approximate line. Note that the simulated results of the highly loaded edge e_{13} are very close to the Gaussian line, while those of e_1 get rather far from it, which would seem to confirm that the load on e_{13} follows a near-Gaussian distribution while the load on e_1 does not.

This is further confirmed by the Lilliefors test for goodness of fit to a Gaussian distribution [30]. The Lilliefors test accepts the hypothesis of e_{13} being a Gaussian (the test is even significant at the stringent 1% level). On the contrary, it rejects the hypothesis of e_1 being a Gaussian (even at the loose 20% significance level). Therefore, both tests confirm that one edge T-Plot displays a Gaussian behavior, while the other does not.

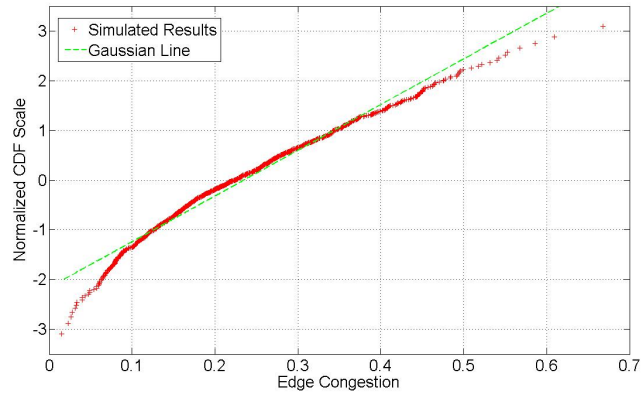
The next Section explains the origin of the different behaviors of the edge T-Plots of e_{13} and e_1 .

4.4 To be or not to be (Gaussian)

While it is clear that both T-Plots display different Gaussian behavior, it is yet unclear why this is the case. In the remainder, we will provide some limited intuition on the factors that might make a distribution Gaussian or not — but stress that we do not provide any



(a) edge e_{13}



(b) edge e_1

Figure 4.2: Normal Probability Plots of the congestion on two edges in Abilene network (the T-Set is \mathcal{A})

simple characterization, which is left for future studies. For simplicity, we will also assume that we have single-path routing.

4.4.1 When flows are i.i.d.

Assume for a moment that flows (i, j) are i.i.d. (independent and identically distributed). In other words, when choosing a traffic matrix D uniformly at random from the T-Set, the distributions of D_{ij} and D_{kl} are i.i.d. whenever the two flows (i, j) and (k, l) are distinct. This might happen, for instance, if the T-Set is defined as the set of all random matrices D such that for all i, j , $0 \leq D_{ij} \leq \frac{1}{n}$. Then, by the central limit theorem, when plotting the T-Plots on links with an increasing number of flows crossing them, the load distribution will become increasingly close to a Gaussian distribution. This is because the load on a link e equals $\sum_{i,j} D_{ij} f_{ij}(e)$. Thus, if there are k flows going through a link, the load can be modeled as the sum of k i.i.d. random variables, which becomes increasingly Gaussian as k grows, with a difference bounded by Berry-Esseen-type bounds [20].

Note that in our typical T-Sets \mathcal{A} , \mathcal{S} and \mathcal{P} , while distinct flows are identically distributed, they are certainly not independent, since there are additional constraints on the row and column sums of the flow values.

Please recall that we assumed a single-path routing. In case of multi-path routing, the mutual dependencies between the various flows crossing each edge become more complex. It is hard to determine whether switching from single-path routing to multi-path routing would either increase or decrease the "entropy", i.e. the rate of independence between different flows crossing the same edge.

4.4.2 A counter-example

Although the above explanation provided some intuition on the Gaussian behavior, we will now show that bad cases might still easily happen, even when n grows to infinity. Assume that in a given network, node 1 sends traffic to $p \cdot n$ destination nodes by using some unit-capacity edge e , and does not use e to send traffic to the other nodes, with $0 < p < 1$ and $p \cdot n$ an integer number. Further assume that no other flow uses e , and that the T-Set is \mathcal{P} , the set of permutation traffic matrices.

The matrix $f(e)$, which determines which (source, destination) pairs route via e , contains $p \cdot n$ ones in the first row and zeros elsewhere. For instance, if $p \cdot n = 3$ then $f(e)$ is:

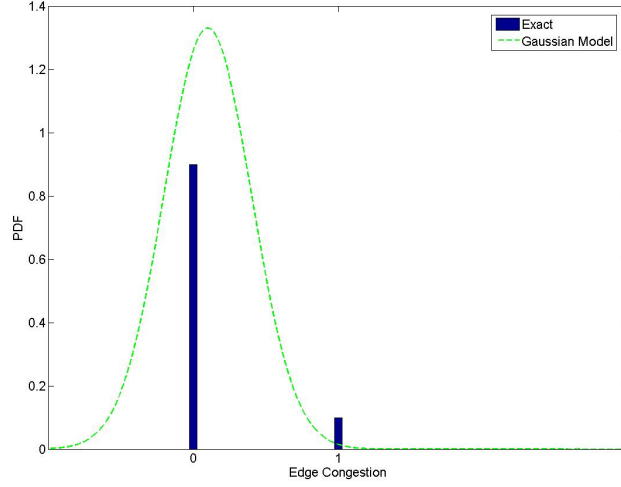


Figure 4.3: PDF of the congestion for the scenario detailed in Sec. 4.4.2 (the T-Set is \mathcal{P})

$$(4.4.12) \quad f(e) = \begin{pmatrix} 1 & 1 & 1 & 0 & 0 & \dots & 0 \\ 0 & 0 & 0 & 0 & 0 & \dots & 0 \\ \dots & \dots & \dots & \dots & \dots & \dots & \dots \\ 0 & 0 & 0 & 0 & 0 & \dots & 0 \end{pmatrix}$$

A fraction p of the permutation matrices will generate a load of 1 on e , and a fraction $1 - p$ a load of 0. The T-Plot PDF will be equal to 1 w.p. p , and 0 otherwise, as shown in Figure 4.3 when $p = 0.1$. The Gaussian model will be generated by a Gaussian random variable of mean p and variance $p(1 - p)$. As Figure 4.3 shows, the Gaussian model is clearly far from the real PDF, and normalizing to have the modeled values at 0 and 1 add up to 1 clearly does not help.

Since this example is valid for all n , it teaches us that even when the number of nodes and the number of flows passing through a link go to infinity, the T-Plot can still *not* converge to a Gaussian distribution. Therefore, much caution must be used. In this case, it seems that this counter-example is possible because of the high dependence between the flows that go through the edge e - dependence which is reflected by the fact that all the non-zero values in $f(e)$ belong to the same row. Note that this dependence does not decrease with n .

4.4.3 When the edge is overloaded

The counter-example given in Section 4.4.2 represents a rather "synthetic" scenario, where an edge is used only for carrying some of the traffic of a single node. In real networks, the overloaded edges tend to be located close to the "center", thus carrying flows of many different nodes. As a consequence, the distribution of the non-zero entries in $f(e)$ would be closer to uniform, and the mutual dependencies between the various flows crossing edge e would decrease. This may give some intuition why the T-Plot of edge e_{13} (Figure 8.4(b)), which is a "central" overloaded edge in Abilene network tends to be much better modeled as Gaussian than the T-Plot of edge e_1 (Figure 4.1), which is a rather "peripheral" under-loaded edge (see description of Abilene network architecture in Chapter 8.2).

Chapter 5

Congestion guarantees

Since it is not guaranteed that Gaussian approximations will be correct, we are interested in providing performance bounds that are guaranteed independently of the shape of the T-Plot. Further, we would like to do so when only using the Gaussian parameters (mean and variance). We will now show that it is indeed possible to use these parameters to provide a bound on the probability that a given edge would achieve less than 100% throughput.

Once we computed the average and the variance of the edge congestion, it is possible to bind the probability that a given edge would achieve less than 100% throughput. This technique is useful both for dynamically identifying of bottlenecks [26], and for online routing algorithms, which try to minimize the interference between possible future demands, such as MIRA [27].

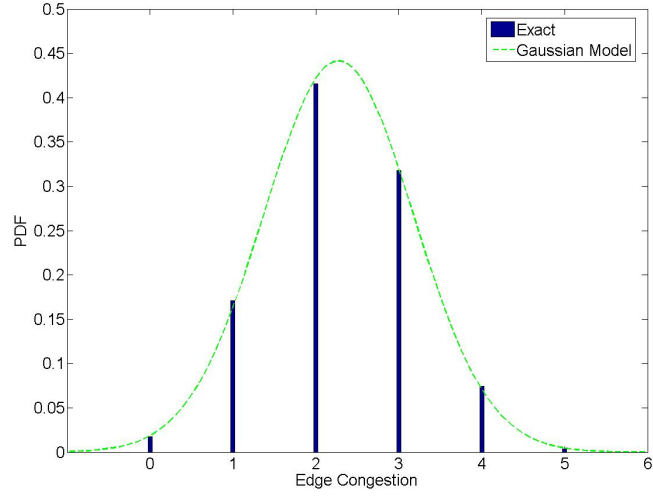
Performance bounds – Let us denote the average edge congestion by μ , and its standard deviation by σ . Let X denote the congestion imposed on a given edge e by a traffic matrix D generated u.a.r. on the T-Set. Then, by Chebyshev's one-tailed inequality with $k \geq 0$,

$$(5.0.1) \quad \Pr(X \geq k\sigma + \mu) \leq \frac{1}{1+k^2}$$

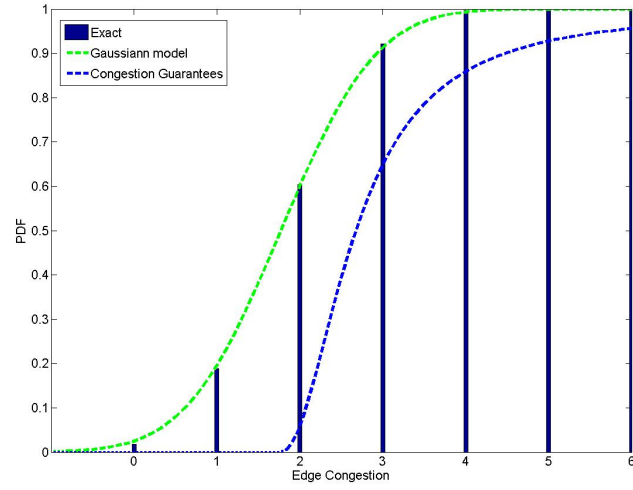
By definition, e is saturated iff $X \geq c(e)$. Therefore, the probability for e to be saturated is upper-bounded:

$$(5.0.2) \quad \Pr(X \geq c(e)) \leq \frac{1}{1 + \left[\frac{c(e) - \mu}{\sigma} \right]^2}$$

Alternatively, given a desired certainty level G , it is possible to calculate a capacity $c'(e)$

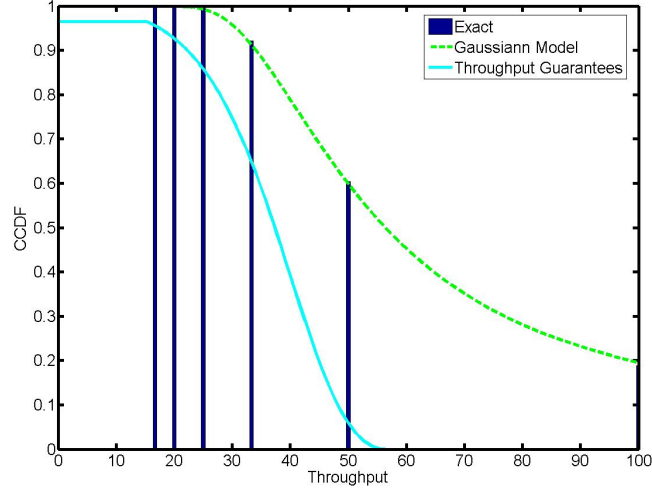


(a) Congestion PDF



(b) Congestion CDF

Figure 5.1: Three views of the same T-Plot (edge 13, the T-Set is \mathcal{P})



(a) Throughput CCDF

Figure 5.2: Three views of the same T-Plot (edge 13, the T-Set is \mathcal{P} , T-Plot of the throughput).

that guarantees that at least a fraction G of the allowable traffic matrices would be served without saturating e . Transforming Equation (5.0.2), we get:

$$(5.0.3) \quad c'(e) = \mu + \sigma \sqrt{\frac{G}{1-G}}$$

Example – Figure 5 provides an example of such a bound. The T-Set is now assumed to be \mathcal{P} , the set of permutation traffic matrices, and the congestion is measured over highly loaded edge e_{13} . Note that Figure 5.1(b) provides three different views of *the same* T-Plot, thus illustrating how a network operator might choose different T-Plots depending on the most significant parameters.

Figure 5.1(a) displays the discrete PDF of the edge congestion together with the Gaussian approximation, which is again extremely close to the exact values (for once, these values are exact, because all the $n!=11!$ permutation matrices were used in the sample).

The same T-Plot is also shown in a CDF form in Figure 5.1(b), together with the new performance bound (which didn't make sense to display on a PDF). For each performance guarantee level, the performance bound now guarantees a sufficient corresponding amount of over-capacity.

Finally, the same T-Plot is also shown as the CCDF (Complementary CDF) of the throughput in Figure 5.2(a). For instance, while some 92% of the matrices get a guaranteed

throughput of at least $1/3$, the performance bound can only guarantee this for 65% of the matrices.

Chapter 6

Approximation and bounds of the global congestion CDF

So far, we have mainly dealt with *edge* congestions. We will now deal with *global* congestions. Of course, succeeding to well approximate the *global* T-Plots would mean obtaining a performance model for the whole network. We will first provide a simple approximation assuming independence, and then an upper-bound.

First assuming that all edge congestions are independent, i.e. traffic matrices cause congestion at different links in an independent manner, provides the following approximation:

$$(6.0.1) \quad GC_{CDF}(f, L) \approx \prod_{e \in E} EC_{CDF}(e, f, L)$$

This is unfortunately quite often a poor approximation, and rather plays the role of intuitive lower-bound, since matrices often cause loads in a clearly dependent way. We thus look for an upper bound. A trivial upper bound is obtained by the CDF of the most loaded edge in the network:

$$(6.0.2) \quad GC_{CDF}(f, L) \leq \min_{e \in E} \{EC_{CDF}(e, f, L)\}.$$

Further, if e_1 and e_2 are two edges (e.g. the two most loaded edges in the network, which

could be the two different directions of the same link), then:

$$\begin{aligned}
Pr\{GC > x\} &\geq Pr\{EC(e_1) > x \vee EC(e_2) > x\} \\
&= Pr\{EC(e_1) > x\} + Pr\{EC(e_2) > x\} \\
&\quad - Pr\{EC(e_1) > x \wedge EC(e_2) > x\} \\
&\geq Pr\{EC(e_1) > x\} + Pr\{EC(e_2) > x\} \\
(6.0.3) \quad &\quad - Pr\{EC(e_1) + EC(e_2) > 2x\},
\end{aligned}$$

where $Pr\{EC(e_1) + EC(e_2) > 2x\}$ is equal to $1 - EC_{CDF}(e_{1,2}, 2x)$, using a dummy edge $e_{1,2}$ for which $f(e_{1,2}) = f(e_1) + f(e_2)$. Using $e_{1,2}$, a similar upper bound is obtainable as follows:

$$\begin{aligned}
Pr\{GC \leq x\} &\leq Pr\{EC(e_1) \leq x \wedge EC(e_2) \leq x\} \\
(6.0.4) \quad &\leq EC_{CDF}(e_{1,2}, 2x)
\end{aligned}$$

A stricter upper bound may then be defined as the minimum of the three bounds (6.0.2), (6.0.3) and (6.0.4).

Chapter 7

Capacity allocation scheme

Let's denote by C_i the capacity of edge i , and by μ_i, σ_i the mean and standard deviation of the load on edge i , respectively. We now suggest to allocate to edge i a capacity of $c(i) = \mu_i + k\sigma_i$, where we use the same value of k for all edges. The total capacity required, as a function of k , is:

$$(7.0.1) \quad \sum_{i=1}^{|E|} c(i) = \sum_{i=1}^{|E|} \mu_i + k \sum_{i=1}^{|E|} \sigma_i$$

Note that when the total capacity is constrained to be smaller than the sum of the average-case edge congestions, k is negative.

We will now show that this capacity allocation minimizes the probability that the network is saturated when using two approximation assumptions: first, the loads on different edges are independent; and second, the edge T-Plots obey a Gaussian model with the same standard-deviation.

We remind that a network is saturated if at least one edge in it is saturated; an edge e is saturated if the edge congestion on it is at least 1, i.e. the flow crossing e is not below its capacity.

Theorem 3 *Assume that the T-Plots of all edges i are independent and Gaussian of mean μ_i and same standard-deviation σ . Then allocating to each edge i a capacity $C_i = \mu_i + k\sigma$, where k is a real constant, minimizes the probability that the network is saturated.*

Proof. We denote the total available capacity by C , i.e., a legal capacity allocation satisfies $\sum_i C_i \leq C$. We would like to maximize the probability that the global congestion

is below 1. Formally, we want to find

$$\begin{aligned} & \underset{\{C_1, \dots, C_{|E|}\}}{\operatorname{argmax}} \quad \Pr\{GC(f, C_1, \dots, C_{|E|}) < 1\} \\ & \text{s.t.} \quad \sum_{i=1}^{|E|} C_i = C \end{aligned}$$

Using the independence assumption, we want to maximize the product of the probabilities of edge congestions on all edges:

$$(7.0.2) \quad \Pr\{GC(f, C_1, \dots, C_{|E|}) < 1\} = \prod_{i=1}^{|E|} EC_{CDF}(e_i(C_i), f, 1)$$

Let $H(x)$ be the standard Gaussian CDF, and $h(x)$ the PDF (its derivative). Then,

$$(7.0.3) \quad EC_{CDF}(e_i(C_i), f, 1) = H((C_i - \mu_i)/\sigma).$$

Using Lagrange multipliers and differentiating Equation (7.0.2), we find that the objective function is maximized when for each $i \neq j$,

$$(7.0.4) \quad \frac{EC_{PDF}(e_i(C_i), f, 1)}{EC_{CDF}(e_i(C_i), f, 1)} = \frac{EC_{PDF}(e_j(C_j), f, 1)}{EC_{CDF}(e_j(C_j), f, 1)},$$

i.e.

$$(7.0.5) \quad \frac{h((C_i - \mu_i)/\sigma)}{H((C_i - \mu_i)/\sigma)} = \frac{h((C_j - \mu_j)/\sigma)}{H((C_j - \mu_j)/\sigma)}.$$

Equation (7.0.5) is solved when $C_i = \mu_i + k\sigma$ for each i , where k is *the same* constant for each i , because all the PDF probabilities are then equalized (the standard-deviations are equal) as well as the CDF probabilities. Therefore, this solution maximizes the objective function. Note that for different standard deviations, this Lagrangian-based method can also directly bring the optimal, yet less elegant, capacity allocation solution, by solving Equation (7.0.5) using methods of numerical analysis.

Chapter 8

Simulations

8.1 T-Set representation

We need the ability to pick a traffic matrix u.a.r. from the T-Set for two reasons. First, to obtain a close approximation of the average and the variance of the edge congestion (as explained in Section 4.2.1). Second, to compare the models developed in the previous chapters to simulation results. While it is easy to generate a random permutation, picking a traffic matrix u.a.r. from \mathcal{S} or \mathcal{A} is harder. To do so, we used random-walk sampling. After starting from some matrix in the T-Set (e.g., the null matrix), we computed a new matrix each time. To do so, at each step, we compute the matrix change Δ , and add it to the current matrix D , so that the new matrix is $D' = D + \Delta$. If D' is in the T-Set, we move to it, and reject it otherwise. When the T-Set was \mathcal{A} , we performed a Gaussian version of the ball walk [40], i.e. the next point in the walk is normally distributed around the current point such that $\Delta[i, j] \sim N(0, 1/2n)$ for each i, j (of course, other random-walk approaches can be used if the guaranteed rate of convergence is important to the user, as explained further in [40]). When the T-Set was \mathcal{S} , we picked at each step 4 integers (i_1, j_1, i_2, j_2) u.a.r. from $[1, n]$, generated a normally distributed step $\delta \sim N(0, 1/2n)$, and assigned $\Delta[i_1, j_1] = \Delta[i_2, j_2] = -\delta$ and $\Delta[i_1, j_2] = \Delta[i_2, j_1] = \delta$. The rest of the entries in Δ are zeros. Note that this generation process requires checking at each step whether the next matrix is indeed in the required T-Sets. In any case, speed was not a problem: for instance, it takes a few minutes to generate a million random samples in the Abilene case ($n = 11$) using an unoptimized Matlab script. However, we needed to check that the sample distribution indeed converges, in the expected speed, to the uniform distribution on the T-Set. To do so, we used three different tests.

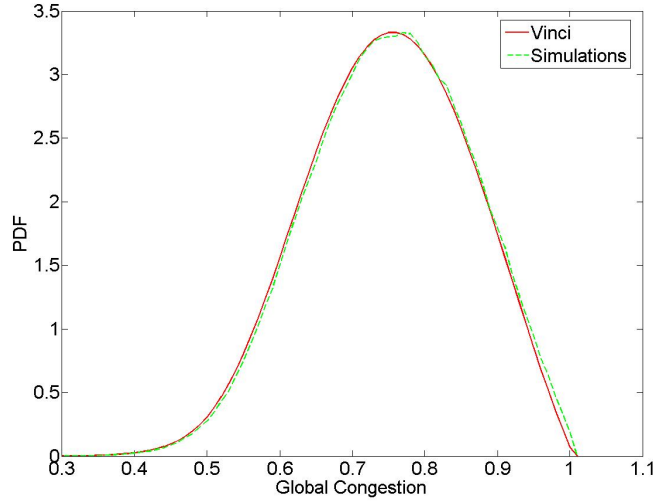


Figure 8.1: PDF of the global congestion in the 2×2 cube (when the T-Set is \mathcal{A})

First, we used the fact that computing the T-Plots when the T-set is \mathcal{A} may also be expressed as a volume computation problem [17]. For each load value L , the region

$$\mathcal{R} = \{D \in \mathcal{A} | GC(f, D) < L\}$$

forms a convex polytope. The ratio between the volume of \mathcal{R} and the volume of the polytope \mathcal{A} is equal to $GC_{CDF}^T(f, L)$. (This method can be extended to \mathcal{S} , as it is possible to compute the volume of \mathcal{S} with n nodes by computing the volume of \mathcal{A} with $n - 1$ nodes [14].) Therefore, we could compare the results of our Monte Carlo simulations using 1 million u.a.r.-generated matrices to the exact results obtained by Vinci [41], a standard convex-polytope volume computation tool. As noted before, computation of the volume of polytopes is $\#P-C$ [18], and therefore we used a small sample network: the 2×2 cube with $n = 4$ and DOR routing [35]. Figure 8.1 is a T-Plot of the global congestion at this network. The graph shows that the simulation results are extremely close to Vinci's exact results.

The comparison with Vinci strongly validates the approach with a small n . However, as n becomes larger, there is no way to verify the results. We checked two other, much weaker properties. First, we checked that the resulting T-Plot is independent of the initial matrix. Second, after m experiments of u.a.r. generated points, we verified that the variance did indeed decrease as $O(1/m)$ and obey the formula $var[X] = \frac{p(1-p)}{m}$, where X is the indicator r.v. representing the fact that the sample is in some bin and $p = EX$.



Figure 8.2: Abilene backbone network

8.2 Experimental setup

We use Abilene as a sample backbone network [1], and provide a simple model of its characteristics. We assume a shortest path routing according to the metric shown in Figure 8.2.

All link capacities are 10Gbps [2]. We further assume that each node can send and receive up to 10Gbps (homogeneous case). Obviously, we may normalize it by using units of 10Gbps; that is, assume that nodes have a unit injection and ejection bandwidth, and that the edge capacities are all equal to 1. We will later revisit this assumption, which is rather pessimistic in the sense that the aggregated rate received or initiated by each of Abilene’s nodes is usually far below 10Gbps [3]. In this Thesis, we focus on the most loaded edge, called e_{13} , which corresponds to the (Kansas City, Indianapolis) directed edge; and on the least loaded edge, called e_1 , which corresponds to the (Seattle, Sunnyvale) directed edge.

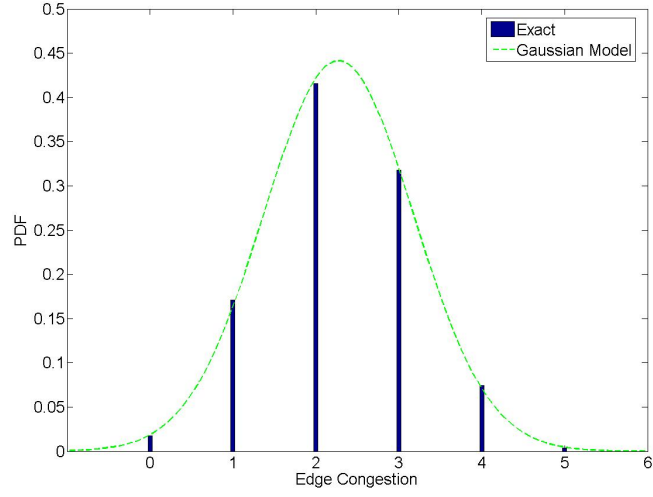
Abilene contains 11 nodes, so the number of permutations is $11!$, and an exhaustive examination is feasible. Thus, the T-Plots for the set of permutations, \mathcal{P} , and for the set of derangements, \mathcal{P}_d , include the exact results. However, when the network contains more nodes, an exhaustive examination is not feasible anymore, and the common method is to use Monte Carlo simulations [37, 33, 38, 34]. Indeed, neither are exact results obtainable when the T-Set is continuous. For such cases, we simulated 1 million u.a.r.-generated traffic matrices, as explained above.

8.3 Edge T-Plots

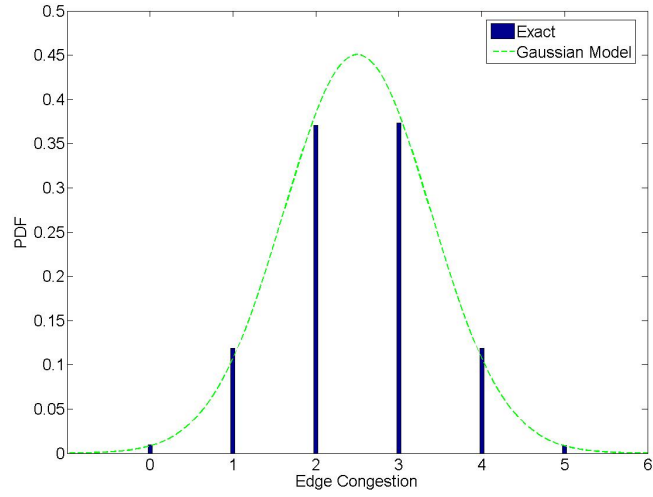
Figures 8.3 and 8.4 show the PDF of the edge congestion on edge e_{13} . Figure 8.3(a) is identical to Figure 5.1(a) which shows the PDF of the edge congestion on edge e_{13} , where the T-Set is \mathcal{P} , and is given here again for convenience. Figure 8.3(b) shows the PDF of the edge congestion on edge e_{13} , where the T-Set is \mathcal{P}_d . The Gaussian approximation for this case is again very accurate. A comparison between Figure 8.3(a) and Figure 8.3(b) shows that the probability of an edge to become congested increases when switching from permutations to derangements, since no efficient routing algorithm would waste network resources to route a packet from a node to itself. This shows how assuming that the traffic matrix belongs to the whole set of permutations, which is often done in the literature [37, 33, 38, 34], is a bit too optimistic. The theoretical computation shows that the ratio between the mean load when the T-Set is \mathcal{P}_d and the mean load when the T-Set is \mathcal{P} is $n/(n-1)$ (see Chapters 4.1 and 4.2).

Figure 8.4(a) shows the PDF of the edge congestion on edge e_{13} , where the T-Set is \mathcal{S} . The Gaussian model fares well again, as in the other T-Plots involving e_{13} . Figure 8.4(b) is identical to Figure 1.1 which shows the PDF of the edge congestion on edge e_{13} where the T-Set is \mathcal{A} , and is given here again for convenience. A comparison between Figure 8.3(a) and Figure 8.4(a) reveals that when switching from \mathcal{P} to \mathcal{S} , the variance of the congestion decreases, which is intuitively explained by the fact that the permutations represent the edge cases, which have a larger tendency to be either extremely overloaded or extremely underloaded. Note that a further decrease in the variance (and also in the average) of the congestion happens when switching from \mathcal{S} (Fig. 8.4(a)) to \mathcal{A} (Fig. 8.4(b)). This decrease happens because \mathcal{A} includes also traffic matrices whose total sum is smaller than n , thus typically representing lower traffic demands, and smaller probability for edge cases.

Figures 8.5 and 8.6 are similar to Figures 8.3 and 8.4 respectively, but now the distributions are plotted for edge e_1 . Figure 8.6(b) is identical to Figure 4.1 which shows the PDF of the edge congestion on edge e_1 where the T-Set is \mathcal{A} , and is given here again for convenience. It can be seen again that there is a continuous decrease in the mean edge congestion when switching from \mathcal{P}_d to \mathcal{P} , further to \mathcal{S} and finally to \mathcal{A} . Note that for none of the plots does the Gaussian Model fare well - see the discussion in Chapter 4.

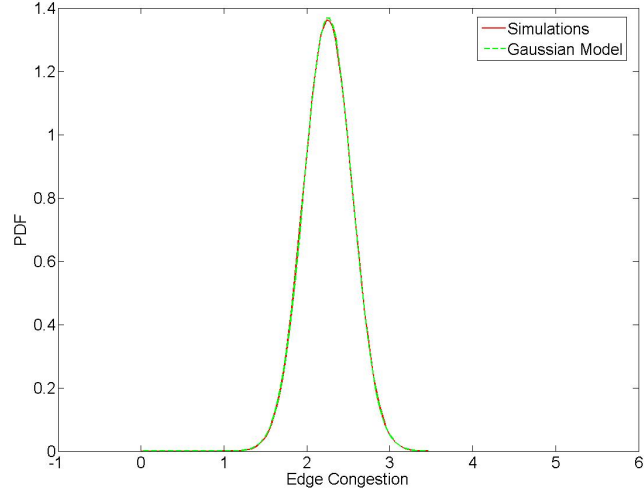


(a) Congestion PDF on e_{13} (over \mathcal{P})

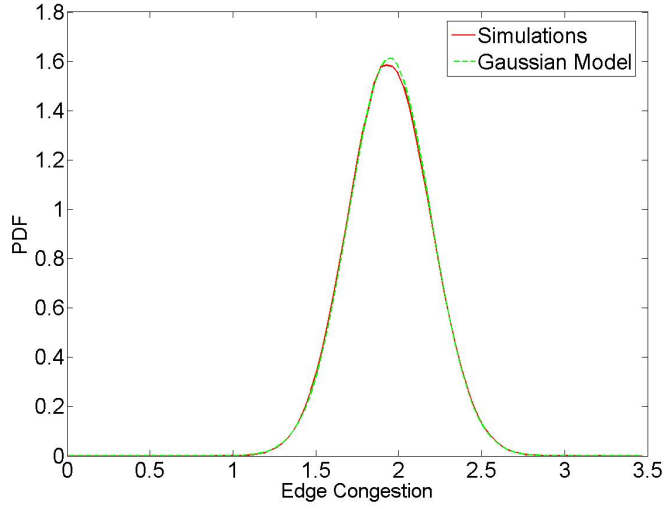


(b) Congestion PDF on e_{13} (over \mathcal{P}_d)

Figure 8.3: Congestion PDF on e_{13} over discrete T-Sets

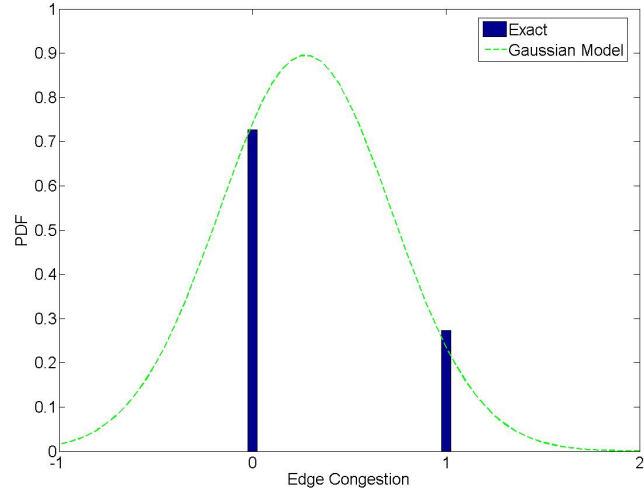


(a) Congestion PDF on e_{13} (over \mathcal{S})

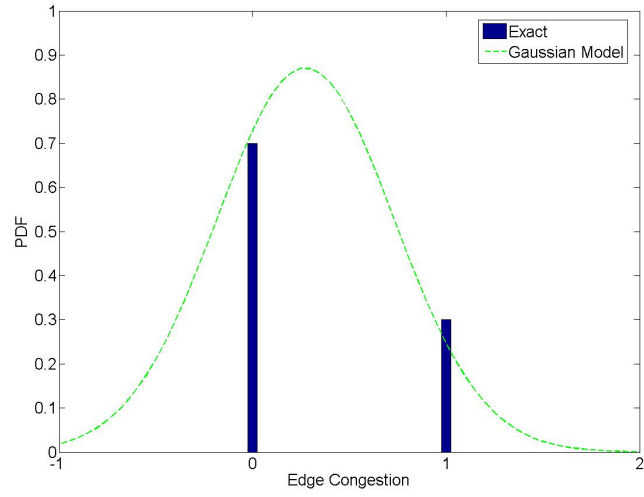


(b) Congestion PDF on e_{13} (over \mathcal{A})

Figure 8.4: Congestion PDF on e_{13} over continuous T-Sets

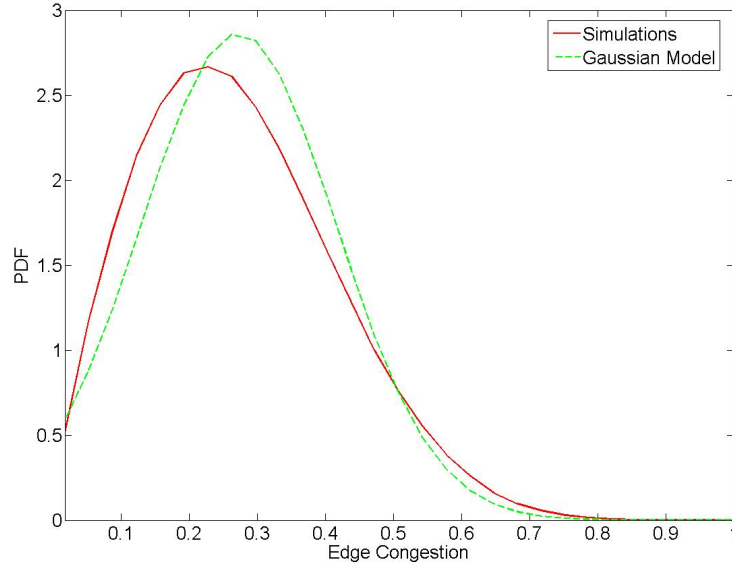


(a) Congestion PDF on e_1 (over \mathcal{P})

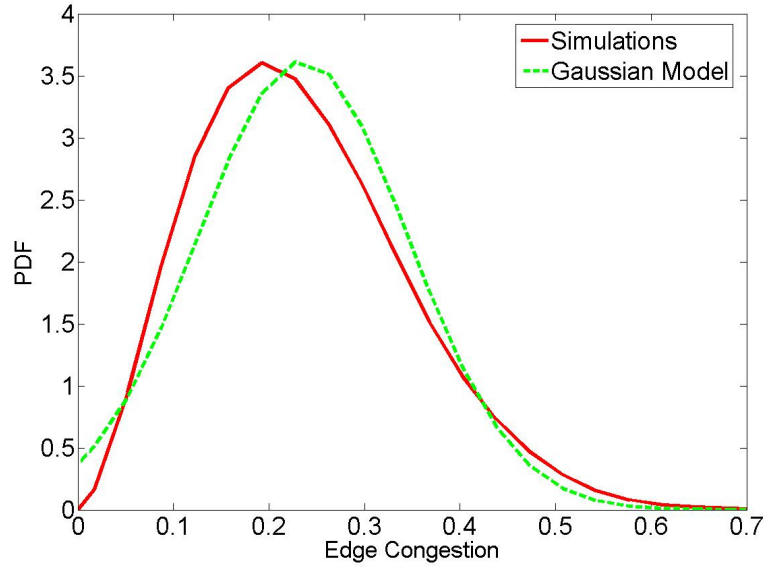


(b) Congestion PDF on e_1 (over \mathcal{P}_d)

Figure 8.5: Congestion PDF on e_1 over discrete T-Sets



(a) Congestion PDF on e_1 (over \mathcal{S})



(b) Congestion PDF on e_1 (over \mathcal{A})

Figure 8.6: Congestion PDF on e_1 over continuous T-Sets

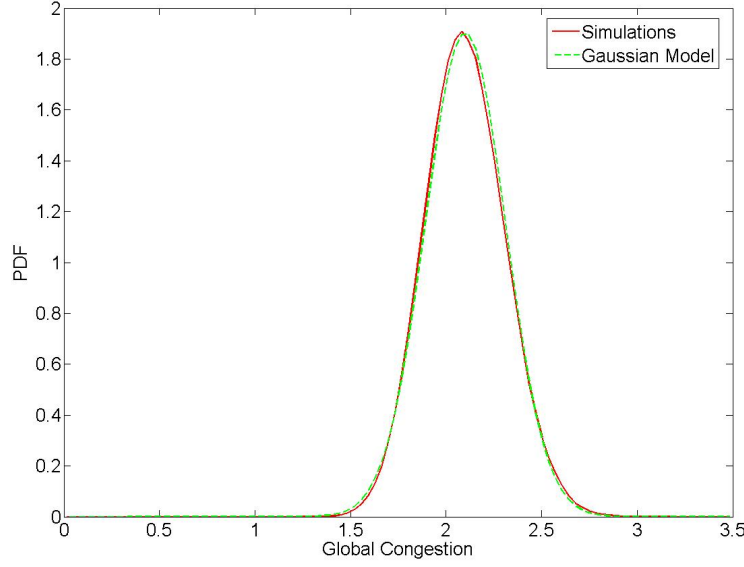


Figure 8.7: Global congestion PDF: over \mathcal{A}

8.4 Global T-Plots

Figure 8.7 shows the PDF of the global congestion in Abilene. It can be seen that it is well fitted by a Gaussian distribution. Note that here, contrarily to all other places, we only fitted the Gaussian distribution without using *a-priori* models. In other words, the mean and the variance of the distribution, which are necessary for plotting the Gaussian, are those found using simulations, and not by theoretical models - as we do *not* have such for *global* T-Plots. Note that the maximum of n i.i.d. Gaussian random variables does *not* behave as a Gaussian random variable (it follows a Gumbel distribution [22]), and thus one must be careful with the conclusions taken from this plot. It is reasonable to assume that most of the Gaussian behavior comes from the few most loaded links, like e_{13} .

Figure 8.8(a) shows the CDF of the global congestion in Abilene. We calculate the approximation and the upper bounds using the models developed in Chapter 6. Note that switching from the Gaussian approximation to the real values to plot the upper bound result in nearly undistinguishable results. The figure shows that both the approximation and the upper bound are rather close to the exact results. The T-Plot directly translates into a required capacity overprovisioning: for instance, since $GC_{CDF}^T(f, 1.5) = 0$, it is necessary to use at least 50% overprovisioning to guarantee that at least some traffic matrices can be services (we remind that we used a pessimistic assumption regarding traffic

demands). Likewise, $GC_{CDF}^T(f, 2.7) = 1$, and so a capacity of 2.7 would guarantee 100% throughput. We will see below that it is possible to guarantee 100% using a much lower overprovisioning, by deploying an optimized capacity allocation.

8.5 Improved capacity allocation

Until now, we realized every T-Plot "as-is", without doing any optimization: we simply measured the distribution of the link load distribution. We will now show that T-Plots can do more than just *measure*: they can also help *optimize*.

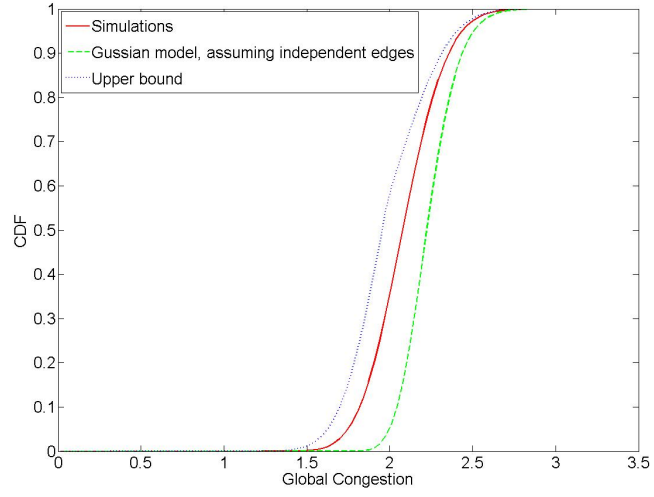
Until now, we have used an homogeneous capacity allocation of the Abilene backbone network. We assumed that the homogeneous Abilene network contains 28 edges, each of unit capacity - i.e. total capacity is 28 units.

We will now assume that capacity can be distributed differently among the edges, so that the total allocation cost is simply equal to the sum of the capacities. Using the simple capacity allocation scheme presented in the Chapter 7, we force $\sum_{e \in E} c(e) = 28$ in Equation (7.0.1), and get $k = 1.14$.

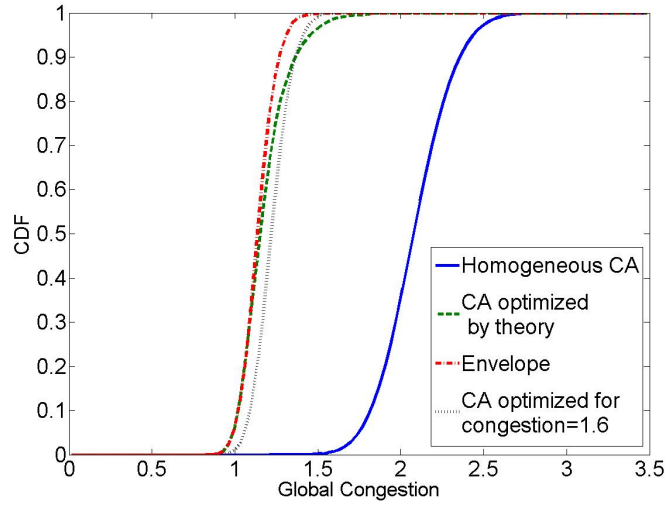
To examine the quality of our capacity allocation scheme, we compare it to an optimized capacity allocation scheme, which was obtained after extensive simulations. Given an optimization criterion, the simulations include 10,000 iterations. At each iteration, a new capacity allocation is taken at the neighborhood of the old one using the Gaussian ball-walk distribution mentioned above (Chapter 8.1), and is only accepted if it fares better. At each point, the throughput was calculated using 10,000 u.a.r.-generated \mathcal{A} matrices. (We also checked that starting from different points yields the same result.)

But what is the optimization criterion? It turns out that optimizing for different values in the global congestion CDF will yield different solutions. Therefore, we performed different optimizations on the whole spectrum of the global congestion CDF. For each value within this spectrum, we maximized the fraction of matrices yielding a global congestion under this value. Thus, we got a full envelope plot indicating an upper bound of the achievable CDF.

This is better understood with Figure 8.8(b), which shows the CDF of the global congestion when using different capacity allocation schemes. First, the homogeneous capacity allocation performs poorly relative to the other capacity allocations. Next, we ran the optimization process described above for the single congestion value of 1.6. While it obtains an optimal allocation for that value, i.e., maximizes the fraction of matrices with a global



(a) Global congestion CDF (over \mathcal{A})



(b) Global congestion CDF, for various Capacity Allocations (over \mathcal{A})

Figure 8.8: Global congestion CDF: bounds and improvements

congestion under 1.6, it is clear that it does not perform optimally elsewhere. Therefore, an allocation scheme that is optimal at one point is not necessarily optimal across the whole spectrum. For this reason, we also determine the envelope plot of optimal values at each point of the spectrum (note that each point of this envelope corresponds to a different scheme; thus this envelope is an upper bound, rather than the performance of a specific allocation scheme). Finally, we show the results of our simple allocation. It clearly performs well, is close to the upper bound, and on most points behaves better than the scheme that is optimal at the congestion value of 1.6. Further, it needs some 40% less capacity than the homogeneous scheme to guarantee most performance levels.

8.6 Heterogeneous network

We finally present a heterogeneous Abilene model taking into account the diverse capacity at each of its nodes. The links still run at 10Gbps links, but different nodes may initiate or receive traffic at different maximum rates. We defined these maximum rates as equal to the maximum rates over a one-day trace, which is publicly available [3]. The T-Plot in Figure 8.9 shows that the global congestion is always far below 1, i.e. Abilene can support all possible traffic demands under this model. Note that the plot has lost the Gaussian behavior found in the homogeneous case (Figure 8.7).

As described in Section 4.2.3, the Gaussian model is also applicable for heterogeneous networks. However, currently, calculating the average and the variance of the edge congestion in such networks requires computing $O(n^4)$ different integrals, and thus we don't present it here. More efficient Gaussian modeling of heterogeneous network is a subject for future research.

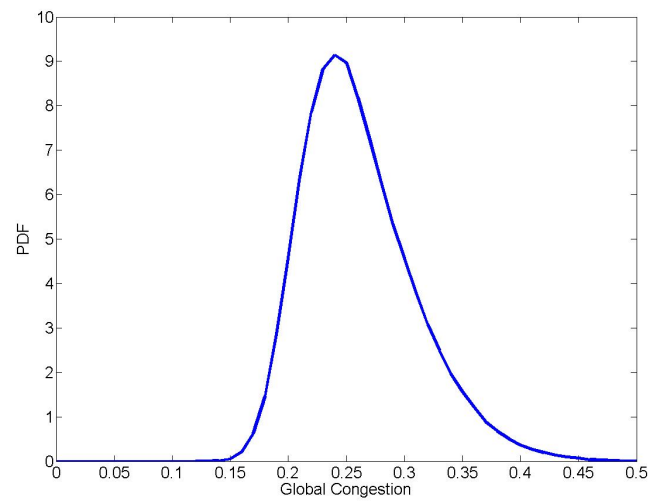


Figure 8.9: PDF of the global congestion for the heterogeneous T-Set

Chapter 9

Conclusion

In this Thesis, we introduced the T-Plots, that can provide a common foundation to quantify, design, optimize and compare traffic engineering algorithms. We also showed that their computation is $\#P$ -Complete, but that they can sometimes be modeled as Gaussian, providing a full link load distribution model using only two variables. Further, we provided bounds that can be the basis of strict throughput performance guarantees. We finally showed how T-Plots can be used to develop a simple, yet efficient, capacity allocation scheme. We believe and hope that this Thesis will contribute to lay the ground to a common basis in future traffic engineering research.

Further, even though we presented our work in the context of backbone networks, it is clear that one can apply it to interconnection networks (such as meshes, hypercubes or bounded-degree graphs), and it would be interesting to study how it relates to the work on oblivious routing in these topologies.

Bibliography

- [1] Abilene backbone network. https://en.wikipedia.org/wiki/Abilene_Network
- [2] Abilene network upgrade. <https://www.internet2.edu/news/detail/1978/>
- [3] Abilene aggregate traffic, daily numbers, accessed in Jan. 2007. <http://www.abilene.iu.edu/abilene/maps-graphs/aggregate-traffic.html>
- [4] S. Agarwal, A. Nucci, and S. Bhattacharyya. Measuring the shared fate of IGP engineering and interdomain traffic. In *Proc International Conference on Network Protocols (ICNP)*, 2005.
- [5] M. Alicherry and R. Bhatia. Pre-provisioning networks to support fast restoration with minimum over-build, In *Proc. Infocom*, pages 164-175, 2004.
- [6] W. B. Ameur and H. Kerivin. Routing of uncertain traffic demands. *Optimization and Engineering*, 6:283-313, 2005.
- [7] D. Applegate, L. Breslau, and E. Cohen. Coping with network failures: routing strategies for optimal demand oblivious restoration. In *Proc. SIGCOMM*, pages 253-264, 2005.
- [8] D. Applegate and E. Cohen. Making intra-domain routing robust to changing and uncertain traffic demands: understanding fundamental tradeoffs. In *Proc. SIGCOMM*, pages 313-324, 2003.
- [9] Y. Azar, E. Cohen, A. Fiat, H. Kaplan, and H. Racke. Optimal oblivious routing in polynomial time. In *Proc. ACM Symposium on theory of Computing*, pages 383-388, ACM Press, 2003.
- [10] A. Ben-Dor and S. Halevi. Zero-one permanent is #P-Complete, a simpler proof. In *Proc. Israel Symposium on Theory of Computing and Systems*, IEEE Press, 1993.

- [11] M. Bienkowski, M. Korzeniowski and H. Racke. A practical algorithm for constructing oblivious routing, In *Proc. ACM symposium on Parallel algorithms and architectures*, pages 24 - 33, 2003.
- [12] G. Birkhoff. Tres observaciones sobre el algebra lineal. *Univ. Nac. Tucuman Rev. Ser. A*, 5:147-151, 1946.
- [13] J. Chambers, W. Cleveland, B. Kleiner, and P. Tukey. Graphical methods for data analysis. Wadsworth, 1983.
- [14] C. S. Chan and D.P. Robbins. On the volume of the polytope of doubly stochastic matrices. *Experimental Mathematics*, 8:291-300, 1999.
- [15] E. W. Dijkstra. A note on two problems in connexion with graphs. *Numerische Mathematik*, 1:269-271, 1959.
- [16] N. Duffield, P. Goyal, and A. Greenberg. A flexible model for resource management in virtual private networks. In *Proc. SIGCOMM*, 1999.
- [17] N. Dukkupati, Y. Ganjali, and R. Zhang-Shen. Typical versus worst case design in networking. HotNets-IV, College Park, November 2005.
- [18] M. E. Dyer. and A. M. Frieze. On the complexity of computing the volume of a polyhedron. *SIAM Journal on Computing*, 17(5):967-974, 1988.
- [19] G. Elekes. A geometric inequality and the complexity of measuring the volume. *Discrete Comput. Geom.*, 1:289-292, 1986.
- [20] C. G. Esseen. Fourier analysis of distribution functions: a mathematical study of the Laplace-Gaussian law. *Acta Math.*, 77(1):1-125, 1945.
- [21] J. Gao, L. Zhang. Tradeoffs between stretch factor and load balancing ratio in routing on growth restricted graphs, In *Proc. ACM symposium on Principles of distributed computing*, pages: 189-196, 2004.
- [22] E. J. Gumbel. Multivariate extremal distributions. *Bull. Inst. Internat. de Statistique*, 37: 471-475, 1960.
- [23] A. Gupta, M. T. Hajiaghayi, and H. Racke, Oblivious network design, In *Proc. ACM-SIAM Symposium on Discrete Algorithms (SODA)*, pages 970-979, 2006.
- [24] M. T. Hajiaghayi, R. D. Kleinberg, T. Leighton, and H. Racke. Oblivious routing on node-capacitated and directed graphs, In *Proc. ACM-SIAM symposium on Discrete algorithms*, pages: 782-790, 2005.

- [25] M. T. Hajiaghayi, R. D. Kleinberg, T. Leighton, and H. Räcke. New lower bounds for oblivious routing in undirected graphs, In *Proc. ACM-SIAM symposium on Discrete algorithms*, pages: 918-927. 2006.
- [26] N. Hu, L. Li, Z. Mao, P. Steenkiste, and J. Wang. Locating internet bottlenecks: algorithms, measurements, and implications. In *Proc. SIGCOMM*, pages 41-54, 2004.
- [27] K. Kar, M. Kodialam, and T.V. Lakshman. Minimum interference routing of bandwidth guaranteed tunnels with MPLS traffic engineering applications. *IEEE Journal on Selected Areas in Communications* 18(12):2566-2579, 2000.
- [28] M. Kodialam, T. V. Lakshman, and S. Sengupta. A simple traffic independent scheme for enabling restoration oblivious routing of resilient connections, In *Proc. Infocom*, pages 2329-2340, 2004.
- [29] M. Kodialam, T. V. Lakshman, and S. Sengupta. Efficient and robust routing of highly variable traffic, In *Proc. Workshop on Hot Topics in Networks (HotNets-III)*, 2004.
- [30] H. Lilliefors. On the Kolmogorov-Smirnov test for normality with mean and variance unknown. *Journal of the American Statistical Association*, 62:399-402, 1967.
- [31] H. Liu and Rui Zhang-Shen. On direct routing in the Valiant load-balancing architecture, IEEE Globecom 2005, St. Louis, MO, November 2005
- [32] M. Roughan, M. Thorup, and Y. Zhang. Traffic engineering with estimated traffic matrices. In *Proc. Internet Measurement Conference*, 2003.
- [33] D. Seo, A. Ali, W. T. Lim, N. Rafique, and M. Thottethodi. Near-optimal worst-case throughput routing for two-dimensional mesh networks. In *Proc. International Symposium on Computer Architecture*, pages 432-443, June 2005.
- [34] A. Singh, W.J. Dally, A.K. Gupta, and B. Towles. GOAL: a load-balanced adaptive routing algorithm for torus networks. In *Proc. 30th Annu. international Symposium on Computer Architecture*, pages 194-205, 2003.
- [35] H. Sullivan and T. R. Bashkow. A large scale, homogeneous, fully distributed parallel machine. In *Proce. Symposium on Computer architecture*, pages 105-117. ACM Press, 1977.
- [36] T. Takeda, R. Matsuzaki, I. Inoue, and S. Urushidani. Network design scheme for virtual private network services *IEICE Transactions on Communications*, E89-B.1:3046-3054, 2006.

- [37] B. Towles and W. J. Dally. Worst-case traffic for oblivious routing functions. *ACM Symposium on Parallel Algorithms and Architectures*, 2002.
- [38] B. Towles, W. J. Dally, and S. Boyd. Throughput-centric routing algorithm design. In *Proc. 15th Annu. ACM Symposium on Parallel Algorithms*, pages 200-209, 2003.
- [39] L. G. Valiant. The complexity of enumeration and reliability problems. *SIAM J. Comput.*, 8(3):410-421, 1979.
- [40] S. Vempala. Geometric random walks: a survey. *MSRI volume on Combinatorial and Computational Geometry*, 2005.
- [41] Vinci, <http://www.lix.polytechnique.fr/Labo/Andreas.Enge/Vinci.html>
- [42] J. von Neumann. A certain zero-sum two-person game equivalent to the optimal assignment problem. *Contributions to the Theory of Games*, Princeton Univ. Press, 2:5-12, 1953.
- [43] H. Wang, H. Xie, L. Qiu, Y. R. Yang, Y. Zhang, and A. Greenberg. COPE: traffic engineering in dynamic networks. In *Proc. SIGCOMM*, pages 99-110, 2006.
- [44] Z. Wang, Y. Wang, and L. Zhang. Internet traffic engineering without full mesh overlaying. In *Proc. Infocom*, 2001.
- [45] T. Ye, H. Kaur, S. Kalyanaraman, K. Vastola, and S. Yadav. Optimization of OSPF weights using online simulation. In *Proc. International Workshop on Quality of Service (IWQoS)*, 2002.
- [46] C. Zhang, Z. Ge, J. Kurose, Y. Liu, and D. Towsley. Optimal routing with multiple traffic matrices: Tradeoff between average case and worst case performance. In *Proc. International Conference on Network Protocols (ICNP)*, 2005.
- [47] C. Zhang, Y. Liu, W. Gong, J. Kurose, R. Moll, and D. Towsley. On optimal routing with multiple traffic matrices. In *Proc. Infocom*, 2005.
- [48] Y. Zhang and Z. Ge. Finding critical traffic matrices. *Proc. of DSN 05*, Yokohama, Japan, June 2005.
- [49] R. Zhang-Shen and N. McKeown. Designing a predictable Internet backbone network. In *Proc. Workshop on Hot Topics in Networks (HotNets-III)*, 2004.
- [50] R. Zhang-Shen and N. McKeown. Designing a predictable Internet backbone with Valiant load-balancing. *Proc. International Workshop on Quality of Service (IWQoS)*, 2005.

- [51] I. Cohen, O. Rottenstreich, I. Keslassy. Statistical Approach to Networks-on-Chip. *Proc. ACM/IEEE NoCS*, pp. 171-180, 2008.
- [52] I. Cohen, O. Rottenstreich, I. Keslassy. Statistical Approach to Networks-on-Chip ((extended version). *Proc. ACM/IEEE NoCS*, Vol. 1. Technical Report TR08, 2008.
- [53] I. Cohen, O. Rottenstreich, I. Keslassy. Statistical Approach to Networks-on-Chip. *IEEE Transactions on Computers (ToC)*, 59(6):748-761, 2010.
- [54] Chudzikiewicz, J., Zielinski, Z. Resources placement in the 4-dimensional fault-tolerant hypercube processors network. *FedCSIS Position Papers*, pp. 69–74, 2013.
- [55] Kassing, S., Valadarsky, A., Shahaf, G., Schapira, M., Singla, A. Beyond fat-trees without antennae, mirrors, and disco-balls. in *Proc. Conference of the ACM Special Interest Group on Data Communication*, pp.281–294, 2017.
- [56] Cohen I., Scalosub G. Queueing in the Mist: Buffering and Scheduling with Limited Knowledge. in *Proc. ACM/IEEE IWQoS*, pp.1-6, 2017.
- [57] Cohen I., Scalosub G. Queueing in the Mist: Buffering and Scheduling with Limited Knowledge. *Computer Networks*, 147:204-220, 2018.
- [58] Cohen, I., E., Gil, Goldstein, M., Sa’ar, Y., Scalosub, G., Waisbard, E. Parallel VM Placement with Provable Guarantees in *Proc. IEEE Infocom WKSHPS*, pp. 1-9 1298–1299, 2020.
- [59] Cohen, I., E., Gil, Goldstein, M., Sa’ar, Y., Scalosub, G., Waisbard, E. Parallel VM Deployment with Provable Guarantees in *Proc. IFIP Networking*, pp. 1-9 2021.
- [60] Cohen I., Gil E., Friedman R., Scalosub G. Access Strategies for Network Caching. in *Proc. IEEE Infocom*, pp.28-36, 2019.
- [61] Cohen I., Gil E., Friedman R., Scalosub G. Access Strategies for Network Caching. in *IEEE Transactions on Networking*, 2020.
- [62] Cohen I., Gil E., Scalosub G. On the Power of False Negative Awareness in Indicator-based Caching Systems. in *Proc. IEEE ICDCS*, pp.28-36, 2021.
- [63] Cohen I., Gil E., Scalosub G. Self-adjusting Advertisement of Cache Indicators with Bandwidth Constraints. in *Proc. IEEE Infocom*, 2021.